

# Effective diffusion in partially filled nanoscopic and microscopic pores

I. ARDELEAN\*, G. FARRHERA<sup>a</sup>, R. KIMMICH<sup>a</sup>

*Technical University from Cluj-Napoca, Physics Department, 400020 Cluj-Napoca, Romania*

*<sup>a</sup>Sektion Kernresonanzspektroskopie, Universität Ulm, 89069 Ulm, Germany*

The contribution of the vapor phase to molecular diffusion in porous silica glasses with nanometer (Vycor) and micrometer (VitraPor#5) pores partially filled with water (polar) or cyclohexane (non-polar) was investigated with the aid of pulsed gradient NMR diffusometry. The effective diffusion coefficient of water in nanometer pores (Vycor) decreases with decreasing filling factor, whereas that of cyclohexane increases due to the vapor phase contribution without exceeding its bulk liquid value. On the other hand the effective diffusion coefficient of cyclohexane in micrometer pores (VitraPor#5) was up to ten times larger than the bulk liquid value. This is in contrast to the effective diffusion coefficient in water which first decreases and then increases upon reduction of the pores filling factor. The experimental diffusion features are well represented by a two-phase liquid/vapor exchange model. It is concluded that the dependence of the effective diffusion coefficient on the pore-filling factor is strongly related to the pore dimension and the polar character of the confined fluids.

(Received November 15, 2006; accepted December 21, 2006)

*Keywords:* NMR, Diffusion, Porous silica glass, Nanoscopic and microscopic pores

## 1. Introduction

Molecular dynamics in liquids under confinement in systems with restricted geometry is known to be very different from that in bulk. Both the geometry of the solid matrix and the interactions with the surface are influencing the molecular dynamics. One of the key parameters that characterize the displacements of molecules under confinement and consequently reflect the molecular dynamics is the self-diffusion coefficient. This parameter can be measured in a completely noninvasive way by nuclear magnetic resonance (NMR) techniques [1].

Variation of the molecular concentration in pores may affect the diffusion process in an appreciable manner [2]. At low filling factors the exchange of molecules between liquid and vapor phase has to be considered in the diffusion process. Providing that some experimental conditions are reached, the liquid vapor exchange may lead to enhancements in the diffusion coefficient up to one order of magnitude [3]. This enhancement is due to four orders of magnitude higher diffusivity of molecules in the vapor phase as compared with the liquid phase (see Table 1). Thus the lower density in the vapor phase is compensated.

In the following the contribution of the vapor phase to molecular diffusion in silica glasses with nanometer (Vycor; mean pore diameter 4 nm) and micrometer (VitraPor#5: mean pore diameter 1 μm; VitraPor#4: mean pore diameter 10 μm) pores partially filled with water (polar) or cyclohexane (non-polar) is investigated with the aid of the field gradient NMR diffusometry technique represented by the pulse scheme shown in Fig. 1. The experimental results will be discussed in the frame of a general two-phase exchange model [4] that is based on a two-region approximation [5]. The experimental diffusion

features will be compared with the description of the theoretical model.

## 2. The two-phase exchange model in NMR diffusometry

In completely filled pore spaces the transport properties of filling fluids are predominantly affected by the geometrical restriction, i.e. the tortuosity and the interaction with the surface. According to Archie's law,  $D = \Phi_t^m D_0$ , the effective diffusion coefficient in the pore space,  $D$ , is reduced by tortuosity effects by a factor  $\Phi_t^m$  relative to its bulk value,  $D_0$  [6]. The quantity  $\Phi_t = V_0 / V_t$  represents the total porosity of the sample.  $V_t$  is the total volume including the matrix and the pore space,  $V_0$  is the pores space volume and  $m$  is an empirical exponent.

In an unsaturated porous sample with polar inner surfaces, the liquid and the vapor phase form two interpenetrating systems of different geometry and porosity. Polar and non-polar adsorbates such as liquid water and cyclohexane, respectively, tend to be distributed in a different way in the pore space depending also on the imbibing degree [7]. In any case, the remainder of the pore volume is filled by air saturated with the respective vapor phase. In this case we have to consider two interpenetrating pore systems of different effective porosities  $\Phi_l = V_l / V_t$  and  $\Phi_v = (V_0 - V_l) / V_t$  for the liquid and vapor phases, respectively (the subscript  $l$  stands for liquid and  $v$  for vapor).

Assuming Archie's law again, the reduced diffusion coefficient in the liquid phase can be written in the form 0

$$D_l = \Phi_l^{m_l} D_{l,0} = \Phi_l^{m_l} \left( \frac{V_l}{V_0} \right)^{m_l} D_{l,0} = \Phi_l^{m_l} f^{m_l} D_{l,0}, \quad (1)$$

where  $f = V_l/V_0$  is the filling factor and  $m_l$  is an empirical exponent specific for the liquid phase and depends both on the sample geometry and the wetting properties of the liquid. The diffusion coefficient in bulk liquid is designated by  $D_{l,0}$ . Eq. (1) thus links the porosity effective for the liquid phase,  $\Phi_l$ , to the sample porosity,  $\Phi_t = \Phi_l + \Phi_v$ .

Diffusion in the vapor phase is governed by collisions among the diffusing molecules themselves (Einstein diffusion) or with the pore walls (Knudsen diffusion). The term "wall" may refer both to liquid-vapor interfaces and to inner surfaces of the solid matrix. Taking Knudsen diffusion into account, the effective vapor diffusion coefficient inside a porous system can be derived by adding the diffusion resistances associated with these two types of collisions, i.e. molecule-wall and molecule-molecule 0:

$$\frac{1}{D_v} = \frac{1}{D_K} + \frac{1}{D_E} \quad (2)$$

$D_K$  and  $D_E$  are the Knudsen and Einstein diffusivities, respectively. Note that  $D_v$  approaches  $D_K$  in the Knudsen limit,  $D_K \ll D_E$ , when molecule-wall collisions dominate. It becomes equal to  $D_E$  in the Einstein diffusion regime,  $D_K \gg D_E$ , where molecule-molecule collisions prevail 0.

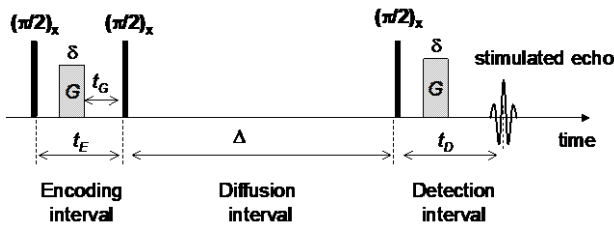


**Fig. 1.** Schematic representation of radio frequency (RF) and field gradient pulse sequence for the stimulated-echo field gradient NMR diffusometry technique.  $G$  represents the spatially constant field gradient along the  $z$ -axis with the duration  $\delta$ .

Anticipating Archie's law again, the quantities  $D_K$  and  $D_E$  can be represented in terms of effective tortuosity factors as above, in order to relate the diffusivities in reduced pore spaces and in "bulk", i.e.,

$$D_K = \Phi_t^{m_{v,K}} (1-f)^{m_{v,K}} D_{K,0}; \quad D_E = \Phi_t^{m_{v,E}} (1-f)^{m_{v,E}} D_{v,0}. \quad (3)$$

The diffusivities in the "bulk" vapor phase are given by  $D_{v,0}$  and  $D_{K,0}$  in the Einstein and Knudsen diffusion limits, respectively. The exponents  $m_{v,K}$  and  $m_{v,E}$  account for tortuosity effects in the Knudsen and Einstein regimes and may consequently also deviate from each other 0.

If we assume that wetting liquids are distributed at the pore walls in the form of a hollow cylinder 0 the diameter of the vapor phase domains can be expressed as a function of the filling factor and the reference Knudsen diffusion coefficient can be written as 0,0

$$D_{K,0}(f) = \frac{1}{3} d (1-f)^{\frac{1}{2}} \sqrt{\frac{8k_B T}{\pi M_0}} \quad (3)$$

Here  $k_B$  is the Boltzmann constant,  $T$  is the absolute temperature,  $M_0$  is the molecular mass, and  $d$  is the mean pore diameter. Note that the reference Knudsen diffusion coefficient is related to the pore shape but may also be different for different chemical species such as water and cyclohexane due to their different wetting properties.

In the following we consider the pulse sequence in Fig.1 where we neglect diffusion, relaxation and exchange phenomena during the encoding interval and assume the spoiling of the transverse magnetization component in the diffusion interval. The combined effect of diffusion, relaxation and exchange on the modulated longitudinal magnetization in the diffusion interval can be evaluated on the basis of a set of "Bloch/Torrey/McConnell equations" (BTC) introduced first in Ref. 0:

$$\frac{dM_{z,l}(z,t)}{dt} = D_l \frac{d^2 M_{z,l}(z,t)}{dz^2} - \frac{M_{z,l}(z,t) - M_{0,l}}{T_{1,l}} - \frac{M_{z,l}(z,t) + M_{z,v}(z,t)}{\tau_l} \quad (4)$$

$$\frac{dM_{z,v}(z,t)}{dt} = D_v \frac{d^2 M_{z,v}(z,t)}{dz^2} - \frac{M_{z,v}(z,t) - M_{0,v}}{T_{1,v}} - \frac{M_{z,v}(z,t) + M_{z,l}(z,t)}{\tau_v}$$

$T_{1,l}$  and  $T_{1,v}$  are the longitudinal relaxation times in the liquid and vapor phase, respectively, in the absence of exchange.  $M_{0,l}$  and  $M_{0,v}$  are the corresponding equilibrium magnetizations. The mean lifetimes the adsorbate molecules spend in the liquid and vapor phases are denominated by  $\tau_l$  and  $\tau_v$ , respectively. Analogously we allocate effective self-diffusion coefficients  $D_l$  and  $D_v$  to the two fluid phases, as given by Eqs. (1) and (2).

The first terms on the right hand side of Eq. (4) describe molecular transport inside the individual phase, the second terms are accounting for longitudinal relaxation in the absence of exchange and the other terms represent molecular inter-phase exchange rates. As a strong simplification, the BTC equations anticipate that both phases are spread uniformly to the entire pore space. That

is, mutual exchange between the two phases can occur at any position  $z$  without prior need to diffuse to an interface.

The mean lifetimes  $\tau_l$  and  $\tau_v$  are effective quantities determined by the extensions of the two-phase regions and the molecular mobilities therein. Additional transport resistances at the interfaces may also play a role. The mean lifetimes are related to the relative number (mass fraction) of molecules in the  $i$ -th phase region,  $p_i$ , by

$$p_i = \frac{\tau_i}{\tau_l + \tau_v} \quad (i = l, v) \quad (5)$$

in a similar way as described in Ref. 0. They can be expressed as a function of the filling factor  $f = V_l / V_0$  and of the respective mass densities,  $\rho_l$  and  $\rho_v$ , as follows:

$$p_l = \frac{f}{f + (1-f)(\rho_v / \rho_l)} \quad \text{and} \quad p_v = 1 - p_l. \quad (6)$$

The general solution of BTC equations (4) which can provide us the amplitude of the stimulated echo, has a generally complicated form (see Ref. 0), and is not given here. It can be simplified in some experimental limits to be described in the following.

**a) The fast liquid/vapor exchange limit**  
( $\tau_l \ll \Delta$  and  $\tau_v \ll \Delta$ )

This limit was considered in the literature many times 0-0 and corresponds to large diffusion paths during  $\Delta$ . The amplitude of the stimulated echo is thus attenuated by diffusive displacements according to 0

$$\frac{A_{STE}(k, \Delta)}{A_{STE}(0, \Delta)} = \exp[-k^2 D_{eff} \Delta] \quad (7)$$

In this case, the effective diffusivity,  $D_{eff}$ , that characterizes the decay, is the weighted average between the diffusion coefficients in the two phases, i.e.,

$$D_{eff} = p_l D_l + p_v D_v \quad (8)$$

The coefficients  $D_l$  and  $D_v$  are given by Eqs. (1) and (2), respectively, and are reduced relative to the bulk values due to the pore space confinement.

**b) The general liquid/vapor exchange description**

For vapor/liquid phase systems we always have

$$p_v \ll p_l; \quad D_v \gg D_l; \quad T_{l,v} \gg T_{l,l}, \quad (9)$$

and the stimulated echo amplitude obeys 0

$$\frac{A_{STE}(k, \Delta)}{A_{STE}(0, \Delta)} = \exp\left[-k^2 \left(D_l + \frac{p_v D_v}{k^2 \tau_l p_v D_v + 1}\right) \Delta\right] \quad (10)$$

Here  $k = \gamma G \delta$  represents the “wave number” of the modulated magnetization that is produced by the gradient pulses of strength  $G$  and duration  $\delta$  and  $\gamma$  is the magnetogyric ratio. The relaxation term has been discarded in the above expression because in experiments with constant intervals but variable gradient strength it does not affect the echo attenuation curve apart from a constant reduction factor. Note that Kärger obtained the same expression for the attenuation of the Hahn echo using a different approach 0. An interesting feature of Eq. (10) is that the mean lifetime,  $\tau_l$ , the molecules spend in the liquid phase can be determined on this basis.

Eq. (10) suggests that no effective diffusion coefficient can be defined since the term in parentheses depends on the wavenumber as a parameter varied in the experiments. However, for small gradient pulse areas complying with the limit  $k^2 \tau_l p_v D_v \ll 1$  one may define  $D_{eff} = D_l + p_v D_v$  as an effective diffusivity with some similarity to the fast-exchange version described below. The initial part of echo attenuation curves can be thus fitted by the mono-exponential decay function

$$\frac{A_{STE}(k, \Delta)}{A_{STE}(0, \Delta)} = \exp[-k^2 (D_l + p_v D_v) \Delta] \quad \text{for} \quad k^2 \tau_l p_v D_v \ll 1. \quad (11)$$

**c) The slow liquid/vapor exchange limit**  
( $\tau_l \gg \Delta$  and  $\tau_v \gg \Delta$ )

In the slow exchange limit when molecular exchange can be neglected on the time scale of the experiment, the attenuation of the amplitude of the stimulated echo by diffusion is characterized by a superposition of two exponentials corresponding to the two phases:

$$\frac{A_{STE}(k, \Delta)}{A_{STE}(0, \Delta)} = p_l \exp(-k^2 D_l \Delta) + p_v \exp(-k^2 D_v \Delta). \quad (12)$$

The diffusion coefficients  $D_l$  and  $D_v$  in the liquid and vapor phase, respectively, are reduced due to the pore space confinement (see Eqs (1) and (2)). Due to the fact that the number of spins in the vapor phase is usually much smaller than in the liquid phase,  $p_v \ll p_l$ , the only component that will contribute to the signal is the liquid component and no contribution from the vapor phase is expected to be perceptible in this limit. Consequently the effective diffusion coefficient that will be measured in this limit is  $D_{eff} = D_l$ .

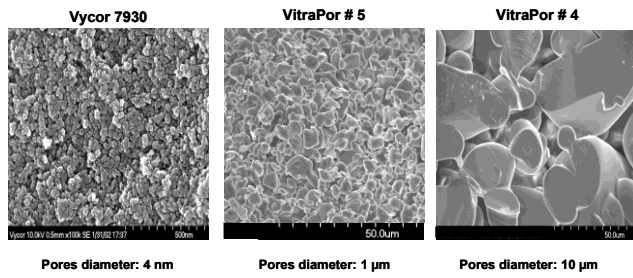


Fig. 2. Electron micrographs of the porous samples used in our experiments. The Vycor sample (4 nm pores) reveals fast exchange between liquid and vapor phase. The VitraPor#5 (1  $\mu\text{m}$  pores) sample reveals the general exchange mechanism and VitraPor#4 (10  $\mu\text{m}$  pores) reveals both the slow and general exchange mechanism.

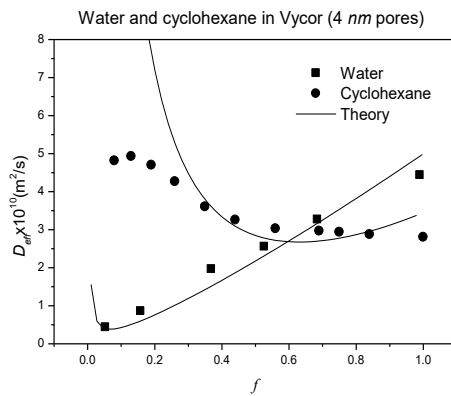


Fig. 3. Effective diffusion coefficients at room temperature for water (squares) and cyclohexane (circles) in Vycor as a function of the filling factor. The data have been extracted from the echo attenuation curves which were mono-exponential functions corresponding to the “fast exchange” limit. The solid lines represent fits of the effective diffusion coefficient given by Eq.(8) to the data. The fitting parameters:

$$m_l^{\text{cyclohexane}} = m_{v,E}^{\text{cyclohexane}} = 1.1; m_{v,K}^{\text{cyclohexane}} = 0.01;$$

$$m_l^{\text{water}} = m_{v,E}^{\text{water}} = 1.2; m_{v,K}^{\text{water}} = 2.0.$$

### 3. Experimental

#### 3.1. Samples and instrumentation

Vycor porous glass VPQ # 7930 was purchased from Corning Ltd. It consists of 96 %  $\text{SiO}_2$ . The nominal mean pore size is  $d = 4 \text{ nm}$  ( $\pm 0.6 \text{ nm}$ ). The manufacturer specifies the porosity as  $\Phi_t = 0.28$ . VitraPor#5 and VitraPor#4 porous silica glasses we purchased from ROBU Glasfilter-Geräte GmbH, Germany. The nominal mean pore size is  $d = 1 \mu\text{m}$  ( $\pm 0.6 \mu\text{m}$ ) and  $d = 10 \mu\text{m}$  ( $\pm 6 \mu\text{m}$ ) respectively. The porosity was measured as  $\Phi_t = 0.43$  and  $\Phi_t = 0.35$  respectively.

The electron micrographs of the three samples are shown in Fig. 2.

The samples were pretreated as suggested by the manufacturer. This includes 30 minutes of boiling in 30 %  $\text{H}_2\text{O}_2$ . The samples were then washed with distilled water and left in vacuum for 24 hours at 95  $^\circ\text{C}$ . After that, the samples are considered to be dry with a nominal filling factor of  $f = 0$ . The solvents were then filled into the porous glass with the aid of the bulk-to-bulk method resulting in a filling factor 1 for the corresponding solvent.

The solvents examined in this study were cyclohexane (non-polar; non-wetting) and demineralized water (polar; wetting). Partial evaporation was then used for the adjustment of the desired filling factor. This was performed in a glove bag in a dry nitrogen atmosphere (for VitraPor#5 sample) in order to avoid any undesired contamination by water from the air humidity. The solvent content reached by this procedure was determined by weighing. The samples were placed in a sealed container with practically no empty space that would allow for further evaporation. All experiments were done only after about one hour permitting the fluid to equilibrate with respect to phase distributions. After this annealing period no changes were perceptible any longer.

All diffusion experiments were performed with a Bruker DPX 400 NMR spectrometer equipped with a microscopy gradient unit. The data were recorded at room temperature and at a proton resonance frequency of 400 MHz using the standard pulsed field gradient stimulated echo technique in Fig. 1 0. The gradient calibration was done with the aid of diffusion measurements in bulk water.

#### 3.2. Results

Fig. 3 shows the effective diffusion coefficient for a diffusion time of 300 ms measured in the case of water (squares) and cyclohexane (circles) partially filling Vycor (4 nm pores) sample. The echo decays (not shown) were always mono-exponential. Consequently the “fast exchange” limit applies in this case and effective diffusion coefficients can be extracted as indicated in Fig. 3. The fitting of the experimental results (solid lines) with an effective diffusion coefficient given by Eq. (8) indicates different tortuosity effects on the Knudsen diffusion contribution in the case of water (squares) and cyclohexane (circles). The fitting parameters are indicated in figures caption. Other physical parameters used in these evaluations were taken from the literature 0, 0 and are indicated in Table 1. The deviation of the theoretical curve, in the case of cyclohexane filled sample, from the experimental data can be due to residual water adsorbed from the air, which could not be removed by the procedure described above. Another possible explanation is the change of the vapor phase density introduced by the interactions with the surface for low filling factors 0.

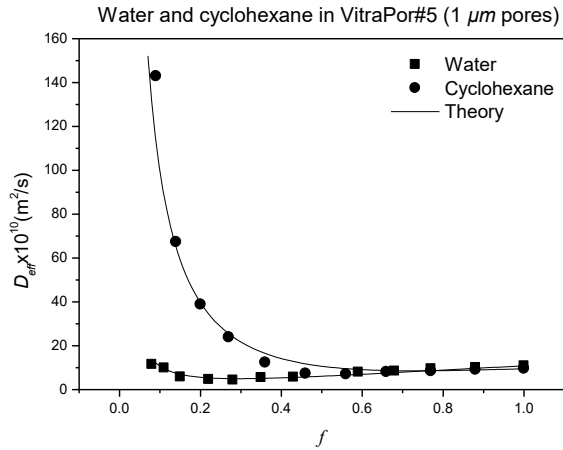


Fig. 4. Effective diffusion coefficients at room temperature for water (squares) and cyclohexane (circles) in VitraPor#5 as a function of the filling factor. The data have been extracted from the echo attenuation curves by fitting a mono-exponential function (see Eq.(11)) to the initial (low wave-number) section. The solid lines represent fits of the effective diffusion coefficient  $D_{eff} = D_l + p_v D_v$  to the data. The fitting parameters are:  $m_{v,E}^{cyclohexane} = m_{v,E}^{water} = 1.4$ ;  $m_{v,K}^{cyclohexane} = 2.2$ ;

$$m_{v,K}^{water} = 3.2; m_l^{cyclohexane} = 0.5; m_l^{water} = 0.87.$$

Fig. 4 shows the effective diffusion coefficient for a diffusion time of 200 ms measured in the case of water (squares) and cyclohexane (circles) partially filling VitraPor#5 (1  $\mu\text{m}$  pores) sample. The echo attenuation curves (not shown) recorded for different filling factors of VitraPor#5 (1  $\mu\text{m}$  pores) were not mono-exponential functions. The decay curves could only be described on the basis of Eq. (10) by assuming the “general liquid/vapor exchange” model given above. Based on Eq.(11), effective diffusion coefficients can be extracted from the “initial” slope of the attenuation curve corresponding to the low wave-number limit,  $k^2 \tau_l p_v D_v \ll 1$ . The data for the effective diffusion coefficients of water (squares) and cyclohexane (circles) are plotted in Fig. 4 as a function of the filling factor. The theoretical curves are also indicated (solid lines). The different dependencies found for water and cyclohexane are attributed to the different vapor pressures 0 and the different surface interactions these two adsorbate species are subject to. The surface interaction is implied in the Knudsen term in Eq.(2) which turned out to be important especially for water. The optimal parameters for the fitting are indicated in figures caption:

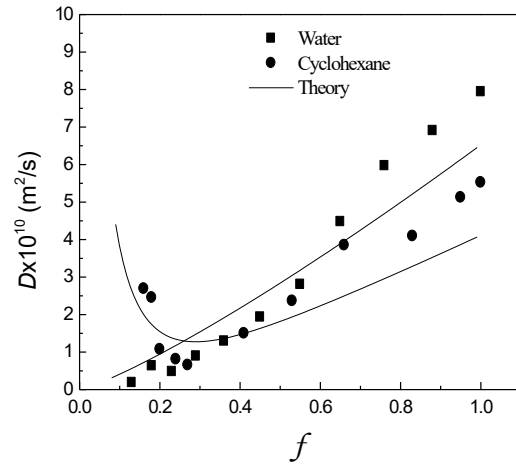


Fig. 5. Effective diffusion coefficients at room temperature for water (squares) and cyclohexane (circles) in VitraPor#4 as a function of the filling factor. The echo attenuation curves were mono-exponential in the case of water corresponding to the “slow exchange” limit. The effective diffusion coefficient is given in this case by  $D_l$ . The case of cyclohexane can be described in the “general liquid vapor exchange” formalism where the effective diffusion coefficient  $D_{eff} = D_l + p_v D_v$  can be defined. The solid lines represent fits of the effective liquid diffusion coefficient, to the data. The fitting parameters are:  $m_{v,E}^{cyclohexane} = 4.1$ ;  $m_l^{cyclohexane} = 1.2$ ;  $m_l^{water} = 1.2$ . No Knudsen diffusion effects are observed in this case.

The “slow liquid-vapor exchange” regime was observed in the case of VitraPor#4 (10  $\mu\text{m}$  pores) sample filled with water. The cyclohexane data indicate the “general exchange” regime. This is due to the higher vapor pressure of cyclohexane as compared with that of water. The effective diffusion coefficient for a diffusion time of 200 ms measured in the case of water (squares) and cyclohexane (circles) is rendered in Fig. 5. The comparison with the theory is also indicated (solid lines). Fitting of the experimental data with a single  $m_l$  was not possible in this case. This is due to the fact that the displacements of molecules during the diffusion time are comparable with the pores dimension and the average of the effective diffusivity over many pores is not accomplished here.

#### 4. Discussion and conclusions

Translational diffusion of water and cyclohexane as polar and non-polar solvent species was studied in porous silica glasses with nanometer (Vycor: mean pore diameter 4 nm) and micrometer pores (VitraPor#5: mean pore diameter 1  $\mu\text{m}$ ; VitraPor#4: mean pore diameter 10  $\mu\text{m}$ ) using NMR diffusometry as a function of the filling factor. The general “two-phase exchange model” well describes all experimental features. The results can be further

analyzed into “fast” and “slow” molecular exchange limits between the liquid and vapor phases.

*Table 1. The physical parameters of water and cyclohexane used in the fits of the theory to our experimental data 00.*

	<b>water</b>	<b>cyclohexane</b>
$\rho_v / \rho_l$	$2.5 \times 10^{-5}$	$5.9 \times 10^{-4}$
$D_{l,0}$ (m <sup>2</sup> /s)	$2.3 \times 10^{-9}$	$1.4 \times 10^{-9}$
$D_{v,0}$ (m <sup>2</sup> /s)	$2.4 \times 10^{-5}$	$8.5 \times 10^{-6}$

In the case of Vycor (4 nm pores) a “fast exchange” between the liquid and vapor molecules is present both for water and cyclohexane filling fluids for a diffusion time of 300 ms. The data on VitraPor#5 sample (1  $\mu$ m pores) can be interpreted in the frame of the “general liquid/vapor exchange” formalism, for an experimental time scale of 200 ms. Both the “slow-exchange” limit and “general exchange” regime have been evidenced in the case of partially filled VitraPor#4 sample (10  $\mu$ m pores). One can conclude that the pore dimension and the polar character of the filling liquids play an essential role for the applicable exchange limit.

The vapor phase effect on diffusion as a function of the filling degree was clearly demonstrated in this way. Due to the molecular exchange, the values of the effective diffusion coefficient in the case of cyclohexane in VitraPor#5 sample (1  $\mu$ m pores), exceed the bulk value by a factor of ten for low filling factors. Molecular exchange means that the solvent molecules are intermittently subject to diffusion features in either phase. Translational displacements in the vapor phase are much faster than in the liquid phase and contribute to the enhancement of the effective diffusion coefficient. For diffusion in the vapor phase, two mechanisms can be distinguished, namely ordinary (“Einstein”) and Knudsen diffusion with, possible different, tortuosity effects from the sample structure. Finally, the mean residence time of the solvent molecules in the liquid phase could be evaluated from the fits of the theory to the experimental echo attenuation data.

## Acknowledgments

This work was supported by the Alexander von Humboldt Foundation, the Deutsche Forschungsgemeinschaft and the Romanian MEC.

## References

- [1] I. Ardelean, R. Kimmich, *Annu. Rep. NMR Spectr.* **49**, 43 (2003).
- [2] J. Kärger, H. Pfeifer, E. Riedel, H. Winkler, *J. Coll. Interface Sci.* **44**, 187 (1973).
- [3] F. D’Orazio, S. Bhattacharja, W.P. Halperin, R. Gerhardt, *Phys. Rev. Letters* **63**, 43 (1989).
- [4] R. Kimmich, S. Stapf, P. Callaghan, A. Coy, *Magn. Reson. Imag.* **12**, 339 (1994).
- [5] R. Kimmich, S. Stapf, R.O. Seitter, P. Callaghan, E. Khozina, *Mat. Res. Soc. Symp. Proc.* **366**, 189 (1995).
- [6] I. Ardelean, C. Mattea, G. Farrher, S. Wonorahardjo, R. Kimmich, *J.Chem.Phys.* **119**, 10358 (2003).
- [7] I. Ardelean, G. Farrher, C. Mattea, R. Kimmich, *J.Chem.Phys.* **120**, 9809 (2004).
- [8] R. Valiullin, P. Kortunov, J. Kärger, V. Timoshenko, *J. Chem. Phys.* **120**, 11804(2004).
- [9] J. Kärger, *Ann. Phys. (Leipzig)[7]* **27**, 107 (1971).
- [10] M. Sahimi, *Rev. Mod. Phys.* **65**, 1393(1993).
- [11] S. G. Allen, P. C. L. Stephenson, J. H. Strange, *J. Chem. Phys.* **106**, 7802 (1997).
- [12] O. Geier, S. Vasenkov, J. Kärger, *J. Chem. Phys.* **117**, 1935 (2002).
- [13] J. Kärger, H. Pfeifer, S. Rudtsch, *J. Magn. Reson.* **85**, 381 (1989).
- [13] Landolt-Börnstein, *Zahlenwerte und Funktionen aus Physik, Chemie, Astronomie, Geophysik und Technik*, Vol. II, Part 5, p.552, Springer Verlag, Berlin-Heidelberg-New York, 1969.

\*Corresponding author: arde@phys.ubbcluj.ro